Journal of Inorganic and General Chemistry
ZAAC
Zeitschrift für anorganische und allgemeine Chemie
DOI: 10.1002/zaac.202000108
ARTICLE

Mono-Phosphazenyl Phosphines $(R_2N)_3P{=}N{-}P(NR_2)_2$ – Strong P-Bases, P-Donors, and P-Nucleophiles for the Construction of Chelates

Julius F. Kögel,[a] Sebastian Ullrich,[a] Borislav Kovačević,[b] Sebastian Wagner,[a] and Jörg Sundermeyer*,[a]

Dedicated to Professor Manfred Scheer on the Occasion of his 65th Birthday

Abstract. We present a convenient three-step synthesis of amino substituted phosphazenyl phosphines of the general formula $(R_2N)_3P{=}N{-}P(NR_2)_2$ [NR_2 = $N(CH_2)_4$, $N(CH_2)_5$, $N(CH_2)_6$]. These easily accessible mixed valent compounds display a surprisingly high proton affinity and basicity in the same range as the corresponding Schwesinger diphosphazene $(Me_2N)_3P{=}N{-}P{=}NEt(NMe_2)_2$ (Et-P_2) and Verkade's proazaphosphatrane superbases. Within the central [P^{III}–N=P^{V}] scaffold, the phosphine P^{III} and not the phosphazene N^{III} atom is the center of highest proton affinity, basicity and donor strength. As P-bases, the title compounds display calculated proton affinities between 265.8 (NR_2 = NMe_2) and 274.7 kcal·mol^{-1} [NR_2 = $N(CH_2)_4$] and pK_{BH}^{+} values between 26.4 (NR_2 = NMe_2) and 31.5 [NR_2 = $N(CH_2)_4$] on the acetonitrile scale. As P-nucleophiles, they are key intermediates in the synthesis of hyperbasic bis(diphosphazene) proton sponges, chiral bis(diphosphazene) proton pincers, bisphosphazides, and superbasic P_2-bisylides. Their Staudinger reactions as nucleophile towards 1,8-diazidonaphthalene leading to 1,8-naphthalene-bisphosphazides is described in detail. The donor strength of the title compounds towards fragments [Se] and [$Ni(CO)_3$] is in the same range as that of N-heterocyclic carbenes.

Introduction

Diphosphazenes have become commercially available and valuable synthetic tools in organic chemistry. As strong non-ionic proton acceptors these Schwesinger P_2-bases[1] can be superior to classical metal organic bases. They allow reactions to proceed with less side products and higher chemo- and stereoselectivity. This can be referred to their ability to generate weakly coordinated carbanions[2] such as applied in aldol reactions,[3] in the generation of S-ylides[4] or in sigmatropic rearrangements.[5]

The classical synthesis of Schwesinger P_2-bases does not involve P^{III} intermediates and their Staudinger reaction with azides, mainly because this strategy would involve hazardous alkyl azides.[1] For this reason, phosphazenyl phosphines, that could act as nitrene acceptors did not prominently move into the focus of scientific interest as starting materials in the two principle routes to Schwesinger bases (Scheme 1).[6] However, a report on the preparation of P_1-phosphazene bases via conversion of P^{III} precursors with organic azides was published by *Alexandrova* et al.[7] We demonstrated that the Staudinger reaction between $[(CH_2)_4N]_3P{=}N{-}P[N(CH_2)_4]_2$ and 1,8-diazidonaphthalene yields the bisphosphazene proton sponge P_2-TPPN (Figure 1), the so far most basic representative of the class of chelating superbases.[8] As surprisingly stable intermediates of P_2-TPPN synthesis, the chelating P_2-bisphosphazide P_2-TPPN($2N_2$) and corresponding dimethylamino substituted P_2-HMPN($2N_2$) with their two different binding sites for metal cations or H-bonded substrates were characterized.[9] Finally, mono-phosphazenyl phosphines described in this paper are key intermediates in the synthesis of higher homologues of superbasic P_2-bisylides such as the so far unknown P_2-MHPN (Figure 1).[10]

* Prof. Dr. J. Sundermeyer
E-Mail: jsu@staff.uni-marburg
[a] Fachbereich Chemie
Philipps-Universität Marburg
Hans-Meerwein-Straße
35032 Marburg, Germany
[b] Group for Computational Life Sciences
Rudjer Bošković Institute
Bijenička c. 54
10000 Zagreb, Croatia
Supporting information for this article is available on the WWW under **http://dx.doi.org/10.1002/zaac.202000108** or from the author.

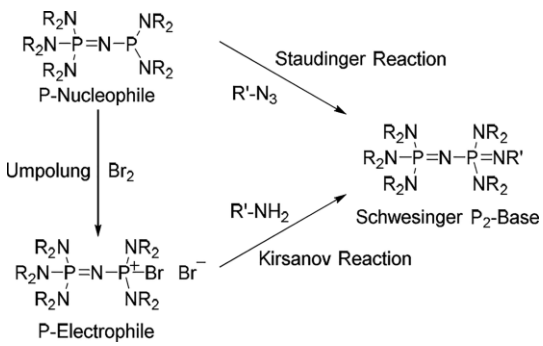

Scheme 1. Synthetic value of the presented P_2-synthons for the preparation of Schwesinger P_2-bases.

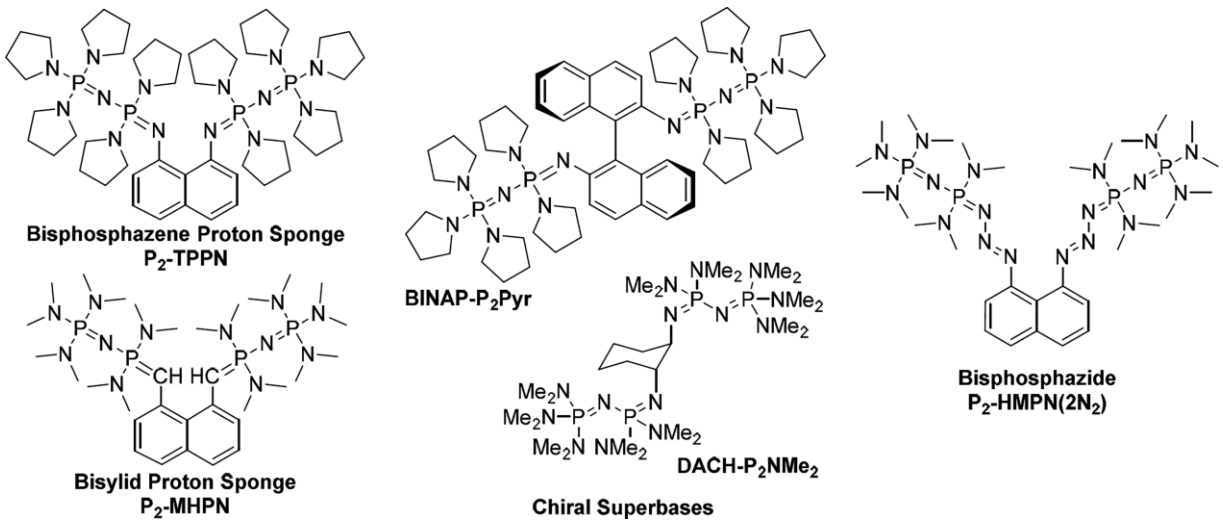

Figure 1. P_2-building blocks in the synthesis of bisphosphazene proton sponge P_2-TPPN,[8] the bisphosphazide P_2-HMPN($2N_2$),[9] chiral superbases[12,13] and superbasic P_2-bisylides.[10]

The second common synthetic strategy towards P_2-phosphazene bases is the Kirsanov reaction[11] which describes the conversion of a primary amine with a P^V-electrophile of the general formula $[(R_2N)_3P{=}N{-}P(NR_2)_2X]^+X^-$ (X = Hal) in the presence of an auxiliary base (Scheme 1). Only recently, we could show the synthetic value of such phosphazenyl phosphine derived P_2-electrophiles $[(Me_2N)_3P{=}N{-}P(NMe_2)_2Br]^+Br^-$ and $[((CH_2)_4N)_3P{=}N{-}P(N(CH_2)_4)_2Br]^+Br^-$ for the preparation of chelating C_2-symmetric chiral superbases with a binaphthyl[12] and a cyclohexyl spacer.[13]

Species with the general formula $(R_2N)_3P{=}N{-}P(NR_2)_2$ exhibit remarkable basicity properties with proton affinities between 265.8 kcal·mol^{-1} for (NR_2 = NMe_2) and 274.7 kcal·mol^{-1} for [NR_2 = $N(CH_2)_4$] – see discussion below. In contrast to most superbases like amidines, guanidines, phosphazenes or proton sponges, the basicity center of the bases presented herein is the P^{III} atom and not the adjacent phosphazene N^{III} atom. This was not only found computationally, but also verified by X-ray crystallographic and NMR spectroscopic methods. Studies concerning the basicity of phosphines have been reported by *Frenking*,[14] *Kolomeitsev*[15] and *Koppel*.[16] One of the best-studied class of P-bases are Verkade's proazaphosphatranes $N(CH_2CH_2NR)_3P$ (e.g. PA = 261.0 kcal·mol^{-1} for R = CH_3).[17] Phosphazene $RN{=}P^V$ derivatives of such phosphatranes have been successfully used as organocatalysts in 1,4-additions of nucleophiles,[18] Stille couplings[19] or the activation of trimethylsilyl cyanide.[20] A very strong P-base, first synthesized as hydrate by *Kirsanov*, but not recognized as superbase for a long time, is $[(Me_2N)_3P{=}N]_3P$ with a proton affinity of 295.5 kcal·mol^{-1}.[17,21] Various other P-bases such as guanidino-substituted $[(Me_2N)_2C{=}N]_3P$ (PA = 278.8 kcal·mol^{-1})[17] exhibit extremely high proton affinity, but have only been isolated in their protonated forms. The corresponding base turned out to be unstable so that their basic properties could only be studied by theory. However, *Dielmann* et al. presented an aromatically stabilized derivative tris(1,3-diisopropyl-4,5-dimethylimidazolin-2-ylidenamino)phosphine (IAP) with an impressive experimental pK_{BH}^+ of 38.8 on the acetonitrile scale.[22,23] Recently, we described higher order tris-phosphazenyl phosphines (tris-PAP) displaying even higher P-basicities than those of IAP or of corresponding Schwesinger N-bases with the same number of P-atoms. At the same time tris-PAP reveal higher Tolman electronic parameters (TEP) than any other neutral P-ligand (Figure 2).[24]

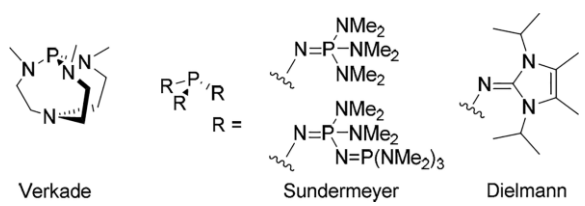

Figure 2. Examples of N-substituted P^{III} compounds with a very high basicity and donor strength.

As tris-PAP tend to be more basic and much stronger donors than needed for catalytic applications we are interested to develop the chemistry of more easily accessible mono-phosphazenyl phosphines $R'_3P{=}N{-}PR_2$ (mono-PAP).

For R = alkyl and phenyl at phosphorus, mono-PAPs have been investigated previously.[25] Much less is known about the all P-amino substituted derivatives put into focus here.

With this publication, we provide deeper insight into the preparation of synthetically most valuable amino-substituted P_2-synthons, their NMR spectroscopic characteristics, their P-basicity and P-donor strength and to some extent also their structural features. A short note on $[(Me_2N)_3P{=}N{-}P(NMe_2)_2Br]^+Br^-$ and the pyrrolidino-substituted compounds $[(CH_2)_4N]_3P{=}N{-}P[N(CH_2)_4]_2$ and $[((CH_2)_4N)_3P{=}N{-}P(N(CH_2)_4)_2Br]^+Br^-$ has been included into the supporting information of our previous communications,[8,9,12,13] but full details of their reactive properties, spectroscopic and structural features as well as their intrinsic basicity and donor strength were not discussed.

Results and Discussion

Synthesis and Spectroscopy of P_2-Synthons

The mixed valent P-nucleophiles of general formula $(R_2N)_3P{=}N{-}P(NR_2)_2$ (**2**–**4**) were prepared via three steps following the strategy laid out for parent $(Me_2N)_3P{=}N{-}P(NMe_2)_2$ (**1**)[21] starting from corresponding phosphorus(III) amides, their Staudinger reaction with TMS-N_3, followed by condensation with PCl_3 and aminolysis of $(R_2N)_3P{=}N{-}PCl_2$ with secondary amines. Oxidation of the P_2-nucleophiles $(R_2N)_3P{=}N{-}P(NR_2)_2$ with bromine leads to an umpolung into P_2-electrophiles $[(R_2N)_3P{=}N{-}P(NR_2)_2Br]^+Br^-$.

$(R_2N)_3P{=}N{-}SiMe_3$ Derivatives

The Staudinger reaction with TMS-N_3 is well documented for the preparation of alkyl- or aryl-substituted species such as $Ph_3P{=}N{-}SiMe_3$,[26] $Me_3P{=}N{-}SiMe_3$[27] or $tBu_3P{=}N{-}SiMe_3$[28] which have been used as precursors for strongly electron-donating phosphiniminato ligands, finally for proazaphosphatrane $N(CH_2CH_2NCH_3)_3P$.[29]

P-amino-substituted derivatives include $(Me_2N)_3P{=}N{-}SiMe_3$,[21,30] $[(CH_2)_4N]_3P{=}N{-}SiMe_3$[31] and $(Et_2N)_3P{=}N{-}SiMe_3$.[32] The stability of initially formed phosphazides $(R_2N)_3P{=}N{-}N{=}N{-}SiMe_3$ with respect to loss of molecular nitrogen depends on the bulkiness of substituents at the phosphorus atom. Whereas $(Me_2N)_3P{=}N{-}N{=}N{-}SiMe_3$ eliminates N_2 at room temperature, phosphazides bearing cyclic amino substituents require heating. *Schlak* et al. reported that a considerable amount of hardly separable P_2-byproduct $(Me_2N)_3P{=}N{-}P(NMe_2)_2{=}N{-}SiMe_3$ is formed in the course of the Staudinger reaction of $(MeN_2)_3P$.[33] We find, that analogous side products are only observed in trace amounts in our compounds with pyrrolidino, piperidino, or azepanyl groups (Scheme 2). The oxidation of the P^{III} atom leads to a strong high field shift in the ^{31}P NMR spectrum. In both, P^{III} amides and P^V amid-imides, an increasing shielding of the phosphorus nucleus is observed in the order $-NMe_2 < -N(CH_2)_6 < -N(CH_2)_5 < -N(CH_2)_4$ (Table 1).

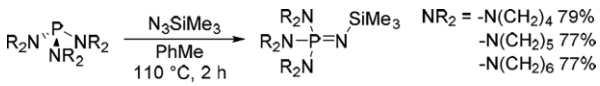

Scheme 2. Preparation of $(R_2N)_3P{=}N{-}SiMe_3$ derivatives.

$(R_2N)_3P{=}N{-}PCl_2$ Derivatives

The second phosphorus atom was introduced via condensation of $(R_2N)_3P{=}N{-}SiMe_3$ with PCl_3 (Scheme 3). The products $(R_2N)_3P{=}N{-}PCl_2$ are isolated in excellent yields as colorless solids. P^V-aryl and P^V-alkyl derivatives of this type were reported by *Eckart* et al. recently.[34]

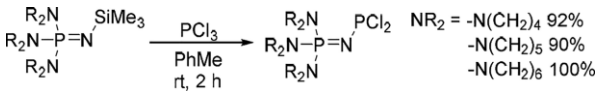

Scheme 3. Preparation of $(R_2N)_3P{=}N{-}PCl_2$.

Compared to the $(R_2N)_3P{=}N{-}SiMe_3$ precursors, the ^{31}P NMR signals of P^V are shifted towards the low field by about 10 ppm while the P^{III} nuclei exhibit nearly equal chemical shifts between 143.0 [R = $N(CH_2)_4$] and 145.2 ppm [R = $N(CH_2)_6$]. Due to the much stronger electron-donating properties of the $(R_2N)_3P{=}N{-}$ substituents, these resonances are found at higher fields compared to corresponding alkyl- and aryl-substituted compounds reported by *Eckart* et al. (e.g. 167.5 ppm in case of $Ph_3P{=}N{-}PCl_2$).[34] The $^2J_{P,P}$ coupling constants range from 81.3 Hz (R = NMe_2) to 88.2 Hz [R = $N(CH_2)_6$] and lie between the values found for $Ph_3P{=}N{-}PCl_2$ (76.3 Hz) and $Cy_3P{=}N{-}PCl_2$ (118.0 Hz)[34] (Table 2).

Table 2. ^{31}P NMR spectroscopic properties [a] of the mixed valent P_2-species $(R_2N)_3P{=}N{-}PCl_2$.

	Yield /%	$\delta_P{}^V$ /ppm	$\delta_P{}^{III}$ /ppm	$^2J_{P,P}$ /Hz
$[(CH_2)_4N]_3P{=}N{-}PCl_2$	92	10.5	143.0	84.6
$[(CH_2)_5N]_3P{=}N{-}PCl_2$	90	17.2	144.5	82.7
$[(CH_2)_6N]_3P{=}N{-}PCl_2$	100	20.6	145.2	88.2
$(Me_2N)_3P{=}N{-}PCl_2$	89	23.1	145.0	81.3

a) All spectra were recorded in [D_6]benzene.

$(R_2N)_3P{=}N{-}P(NR_2)_2$ Derivatives

In case of the piperidino- and azepanyl-substituted species, the substitution of the chlorine atoms of $(R_2N)_3P{=}N{-}PCl_2$ was achieved by the reaction with four equivalents of the corresponding amine in diethyl ether (Scheme 4).

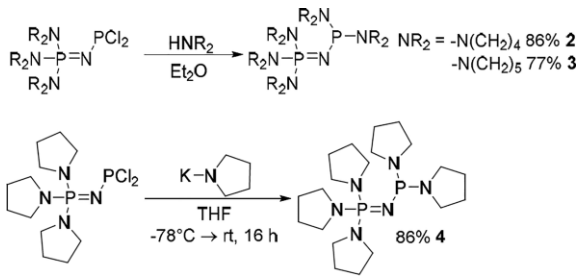

Scheme 4. Synthesis of the title compounds $(R_2N)_3P{=}N{-}P(NR_2)_2$ (**2**–**4**).

Table 1. ^{31}P and ^{13}C NMR spectroscopic data [a] of iminophosphoranes $(R_2N)_3P{=}N{-}SiMe_3$.

	Yield /%	δ_P /ppm	δ_{C1} /ppm	$^2J_{P,C1}$ /Hz	δ_{C2} /ppm	$^3J_{P,C2}$ /Hz	δ_{C3} /ppm	$\delta_{C(TMS)}$ /ppm	$^3J_{P,C3}$ /Hz
$[(CH_2)_4N]_3P{=}NSiMe_3$	79	0.7	46.8	4.3	26.7	7.9	–	5.0	2.7
$[(CH_2)_5N]_3P{=}NSiMe_3$	77	8.4	46.3	1.6	26.9	6.5	25.5	4.8	2.5
$[(CH_2)_6N]_3P{=}NSiMe_3$	77	10.6	48.9	3.7	31.1	5.4	27.3	4.8	2.0
$(Me_2N)_3P{=}NSiMe_3$	57	13.5	37.2	3.5	–	–	–	4.7	2.9

a) All spectra were recorded in [D_6]benzene.

Table 3. ^{31}P NMR spectroscopic properties [a] of the mixed valent P_2-species $(R_2N)_3P{=}N{-}P(NR_2)_2$.

	Yield /%	δ_P^V /ppm	δ_P^{III} /ppm	$^2J_{P,P}$ /Hz
$[(CH_2)_4N]_3P{=}N{-}P[N(CH_2)_4]_2$	86	10.2	93.7	102.1
$[(CH_2)_5N]_3P{=}N{-}P[N(CH_2)_5]_2$	77	17.6	97.3	121.3
$[(CH_2)_6N]_3P{=}N{-}P[N(CH_2)_6]_2$	59	20.0	100.3	118.8
$(Me_2N)_3P{=}N{-}P{-}(NMe_2)_2$	63	22.9	102.1	109.1

a) All spectra were recorded in [D_6]benzene.

Two equivalents of the amine acted as a base with formation of amine hydrochlorides. As the product is more basic than the amine hydrochloride by-product, the lattice energy of precipitating hydrochloride from ether is an essential driving force: In MeCN solution, the product $(R_2N)_3P{=}N{-}P(NR_2)_2$ is fully protonated by $[H_2NR_2]Cl$! Interestingly, this procedure did not work for pyrrolidino derivative $[(CH_2)_4N]_3P{=}N{-}PCl_2$. The desired $[(CH_2)_4N]_3P{=}N{-}P[N(CH_2)_4]_2$ had to be synthesized by reaction of $[(CH_2)_4N]_3P{=}N{-}PCl_2$ with in situ-generated potassium pyrrolidide. Using simple lithium pyrrolidide led to inseparable side products and LiCl base adduct formation. The fully amino-substituted species $(R_2N)_3P{=}N{-}P(NR_2)_2$ are pentane soluble air sensitive colorless oils of extremely high basicity and water affinity. They cannot be purified by column chromatography or vacuum distillation similar to volatile $(Me_2N)_3P{=}N{-}P(NMe_2)_2$. Therefore, their synthesis has to involve most careful inert gas techniques and a final pentane extraction step in order to get spectroscopically pure material.

The substitution of P–Cl for P-amino groups is accompanied by a considerable high field shift of the corresponding ^{31}P NMR signal of formerly P^{III} while the other ^{31}P resonance remains nearly unchanged. The $^2J_{P,P}$ coupling constants are ranging from 81.3 to 121.3 Hz (Table 3). Both, the P^{III} atoms' chemical shifts and the $^2J_{P,P}$ coupling constants in mono-PAPs are significantly lower than their respective tris-PAPs.[24]

In order to get a first impression on the basicity of phosphazenyl-phosphines **1**–**4** an NMR titration experiment using protonated superbasic proton sponge TMGN·HPF_6 was conducted. 1,8-Bis(tetramethylguanidino)naphthalene (TMGN) has experimental and calculated pK_{BH}^+ values in acetonitrile of 25.1[35] and 25.4,[36] respectively. Quantitative deprotonation of TMGN·HPF_6 by $(Me_2N)_3P{=}N{-}P(NMe_2)_2$ was confirmed via ^{1}H and ^{31}P NMR spectroscopy. We did not observe any proton self-exchange between base forms **1**–**4** and corresponding acid forms [**1**–**4**]·HPF_6. In contrast to Schwesinger's phosphazenes, P^{III} bases exhibit significant lower proton self-exchange rates, since a 1:1 mixture of $(Me_2N)_3P{=}N{-}P(NMe_2)_2$ and its corresponding bis(triflyl)imide onium salt showed two separated sets of signals in the ^{1}H and ^{31}P spectra in acetonitrile at room temperature.

$[(R_2N)_3P{=}N{-}P(NR_2)_2Br]Br$ Derivatives

An umpolung of the highly nucleophilic phosphorus(III) atom is achieved by oxidation with bromine in benzene. For P_1-synthons this procedure had been reported by *Issleib* and *Seidel* (Scheme 5).[37] The ionic or non-ionic nature of P_1-species R_3PBr_2 has been disputed in the literature.[38] X-ray crystallography, NMR spectroscopic studies, conductivity measurements and the insolubility in nonpolar solvents revealed that such compounds usually exhibit salt-like character with a $[R_3PBr]^+$ cation and a bromide anion, and not covalent λ^5-phosphorane character. Since such trigonal bipyramidal structure is only found for species with strongly electron-withdrawing substituents like in $(F_5C_6)_3PBr_2$,[38b] the bromophosphonium bromide character is plausible for the compounds treated herein. This has been proven by XRD structure analysis of $[(Me_2N)_3P{=}N{-}P(NMe_2)_2Br]^+Br^-$ (vide infra). Furthermore, only peaks for $[(R_2N)_3P{=}N{-}P(NR_2)_2Br]^+$ cations, but no species containing two bromine atoms were detected in ESI(+) mass spectra from acetonitrile. As expected, P-oxidation is accompanied by high-field shift of δ_P and a strong decrease of the $^2J_{P,P}$ coupling constants (Table 4).

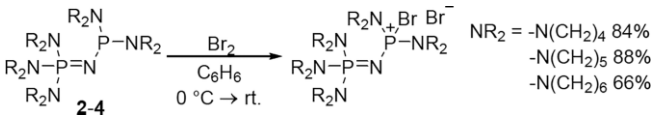

Scheme 5. Umpolung by oxidation of $(R_2N)_3P{=}N{-}P(NR_2)_2$ (**2**–**4**) by reaction with bromine.

A complementary strategy for the preparation of the related P_2-electrophiles $[(Me_2N)_3P{=}N{-}P(NMe_2)_2Cl]^+[BF_4]^-$ and $[((CH_2)_4N)_3P{=}N{-}P(N(CH_2)_4)_2Cl]^+[BF_4]^-$ from $(R_2N)_3P{=}N{-}P(O)(NR_2)_2$ and $POCl_3$ was reported by *Schwesinger* et al.[1]

Reactivity of $(Me_2N)_3P{=}N{-}P(NMe_2)_2$ towards Bis(triflyl) imide

The preparation of thermally highly stable protic ionic liquids containing protonated superbases like phosphazenes or

Table 4. ^{31}P NMR spectroscopic properties [a] of the P_2-electrophiles $[(R_2N)_3P{=}N{-}P(NR_2)_2Br]^+Br^-$.

	Yield /%	δ_P^V /ppm	δ_P^V /ppm	$^2J_{P,P}$ /Hz
$[((CH_2)_4N)_3P{=}N{-}P(N(CH_2)_4)_2Br]^+Br^-$	84	9.9	–5.8	50.3
$[((CH_2)_5N)_3P{=}N{-}P(N(CH_2)_5)_2Br]^+Br^-$	88	14.7	–3.8	56.6
$[((CH_2)_6N)_3P{=}N{-}P(N(CH_2)_6)_2Br]^+Br^-$	66	20.1	–0.9	61.2
$[(Me_2N)_3P{=}N{-}P(NMe_2)_2Br]^+Br^-$	94	23.5	–7.0	54.8

a) All spectra were recorded in [D_3]MeCN.

guanidines as cations and a bis(triflyl)imide anion was reported by *Luo* et al.[39] In this context, we obtain a room temperature ionic liquid of low viscosity by direct protonation of $(Me_2N)_3P{=}N{-}P(NMe_2)_2$ (**1**) with bis(triflyl)imide (HTFSI) in ethyl ether (Scheme 6). The reaction is accompanied by a high field shift of the P^{III} signal and a shift of the $^2J_{P,P}$ coupling constant from 109.1 Hz to 52.4 Hz. The P–H proton exhibits a proton resonance at δ = 6.94 ppm in [D_3]MeCN and a strong $^1J_{P,H}$ coupling constant of 587.4 Hz. Even stronger $^1J_{P,H}$ coupling constants were reported for $[(Et_2N)_3P\text{-}H]^+[BF_4]^-$ (630 Hz), $[((CH_2)_5N)_3P\text{-}H]^+[BF_4]^-$ (632 Hz)[40] or the unstable $[(Me_2N)_3P\text{-}H]^+[OSO_2CF_3]^-$ (680 Hz).[41]

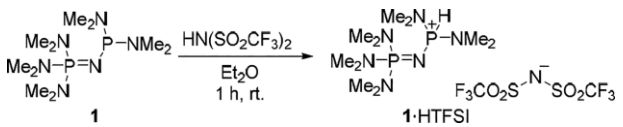

Scheme 6. Reaction $(Me_2N)_3P{=}N{-}P(NMe_2)_2$ (**1**) with bis(triflyl)imide.

Preparation of P_2-Bisphosphazides

The reaction of the mixed valent P^V-P^{III} species $(R_2N)_3P{=}N{-}P(NR_2)_2$ with 1,8-diazidonaphthalene yielded thermally stable P_2-bisphosphazides in a tandem Staudinger reaction. The reaction follows patterns observed for $(Me_2N)_3P{=}N{-}P(NMe_2)_2$ and $[(CH_2)_4N]_3P{=}N{-}P[N(CH_2)_4]_2$.[9] P_2-TPipPN(2N_2) and P_2-TAzPN(2N_2) were obtained as deep green solids in good yields (Scheme 7, Table 5).

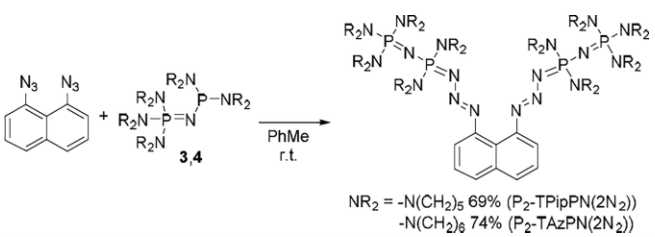

Scheme 7. Preparation of the P_2-bisphosphazides P_2-TPipPN(2N_2) and P_2-TAzPN(2N_2).

Table 5. ^{31}P NMR spectroscopic data of P_2 bisphosphazides.

	Yield /%	δ_P /ppm	δ_P /ppm	$^2J_{P,P}$ /Hz
P_2-TPPN(2N_2) [a) b)]	68	19.7	9.5	48.0
P_2-TPipPN(2N_2) [a)]	69	20.8	15.1	53.5
P_2-TAzPN(2N_2) [a)]	74	23.0	21.8	57.2
P_2-HMPN(2N_2) [b) c)]	85	24.0	19.4	51.7

a) Recorded in [D_6]benzene. b) See reference[9]. c) Recorded in [D_3]MeCN.

They can be clearly distinguished from corresponding superbasic bisphosphazenes by ^{13}C NMR spectroscopy, ESI mass spectrometry, elemental analysis and the typical deep green color of the aryldiazo chromophore. Table 5 summarizes spectroscopic data of P_2-TPipPN(2N_2) and P_2-TAzPN(2N_2) and related P_2-bisphosphazides. From all bisphosphazides presented in Table 5, only P_2-TPPN(2N_2) displayed a thermally or photochemically induced selective N_2 elimination path towards the hyperbasic proton chelating bis-diphosphazene proton sponge P_2-TPPN.[8]

Structural Investigations

Crystal data and experimental conditions of molecular structures presented in the main manuscript are listed in Table S2 (Supporting Information).

$[(CH_2)_5N]_3P{=}N{-}PCl_2$

The compound crystallizes in the orthorhombic space group *Pna*21 with four molecular units in the unit cell (Figure 3). The P–Cl bonds show slightly different lengths of 2.143(1) and 2.181(1) Å and are longer than observed in amino-substituted reference $Me_2N{-}PCl_2$ [P–Cl: 2.091(1), 2.095(1) Å].[42] This fact can be referred of the strongly electron-donating character of the phosphazenyl substituent $[((CH_2)_5N)_3P{=}N{-}]$ and donation of electron density from the nitrogen atom's lone pair into the σ*-P–Cl bond. In accord with this negative hyperconjugation model N4-P2 [1.575(3) Å] is very short for a formal P–N single bond, it is even slightly shorter than N4-P1 [1.592(3) Å] which refers to the formal phosphazene P=N bond. The distances between P1 and the three piperidino nitrogen atoms [1.634(2) to 1.646(2) Å] serve as internal standard for a P–N single bond.[43] A valence bond description $[N_3P^+{-}N{=}PCl]Cl^-$ might best describe the trend induced by negative hyperconjugative interaction. As a consequence, a large angle P1–N4–P2 141.0(1)° is observed.[34]

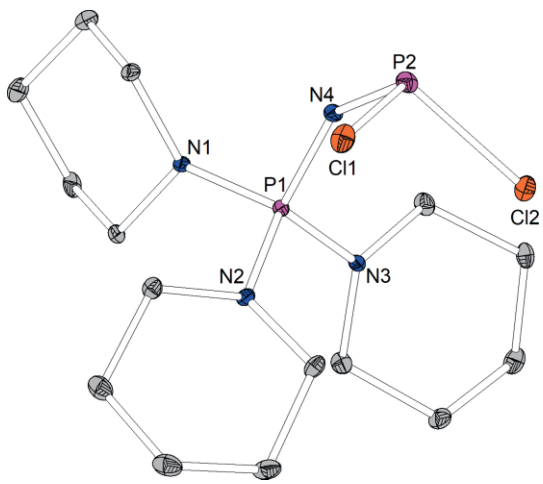

Figure 3. Molecular structure of $[(CH_2)_5N]_3P{=}N{-}PCl_2$ (ellipsoids with 30% probability, hydrogen atoms are omitted for clarity). Selected bond lengths /Å and angles /°: P1–N1 1.646(2), P1–N2 1.638(2), P1–N3 1.634(2), P1–N4 1.592(3), N4–P2 1.575(3), P2–Cl1 2.181(1), P2–Cl2 2.143(1), P1–N4–P2 141.0(1), N4–P2–Cl1 106.45(8), N4–P2–Cl2 106.24(9), Cl1–P2–Cl2 94.38(4).

$[(CH_2)_5N]_3P{=}N{-}P[N(CH_2)_5]_2{\cdot}HCl$ (3·HCl)

3·HCl was obtained as single crystalline material from a product fraction of $[(CH_2)_5N]_3P{=}N{-}P[N(CH_2)_5]_2$ (**3**) in the presence of traces of HCl or piperidine hydrochloride, respec-

tively. **3**·HCl crystallizes in the triclinic space group $P\bar{1}$ with two molecular units in the unit cell (Figure 4). The molecular structure of its hydrochloride proves that the P^{III} atom is the most basic site of $[(CH_2)_5N]_3P{=}N{-}P[N(CH_2)_5]_2$, which was predicted by theory (vide infra). The acidic proton could be located on the Fourier map between basic P2 and Cl2 atoms. The P–H distance of 1.28(3) Å is similar to the corresponding bond length found for $[(CH_2)_4N](t\text{Bu})_2P{\cdot}HBF_4$ [1.29(4) Å].[39]

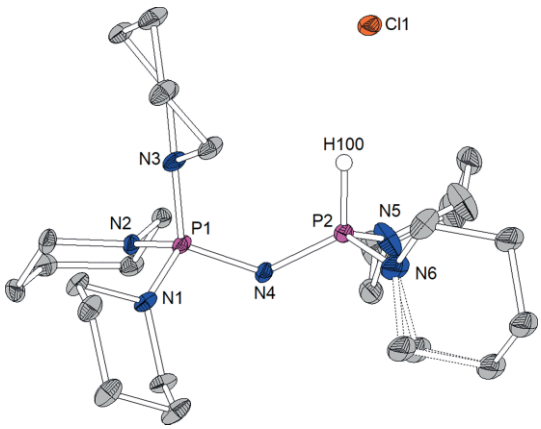

Figure 4. Molecular structure of $[(CH_2)_5N]_3P{=}N{-}P[N(CH_2)_5]_2{\cdot}HCl$ (**3**·HCl) (ellipsoids with 30% probability, carbon bonded hydrogen atoms are omitted for clarity). Selected bond lengths /Å and angles / °: P1–N1 1.638(2), P1–N2 1.639(2), P1–N3 1.640(2), P1–N4 1.584(2), N4–P2 1.576(2), P2–N5 1.622(3), P2–N6 1.632(2), P2–H100 1.28(3), P1–N4-P2 130.1(1).

The H100···Cl1 distance of 2.50(2) Å is below the sum of van der Waals radii (2.85 Å) and indicates a weak interaction between the acidic proton and the chloride anion.[44] The N4–P1 [1.584(2) Å] and N4–P2 [1.576(2) Å] distances are nearly equal and in the range of P–N double bonds, which suggests a delocalization of the positive charge over the PNP system with the three canonical forms $(R_2N)_3P^+{-}N{=}PH(NR_2)_2$, $(R_2N)_3P{=}N^+{=}PH(NR_2)_2$ and $(R_2N)_3P{=}N{-}P^+H(NR_2)_2$. The P1–N4–P2 angle [130.1(1)°] is smaller than in $[(CH_2)_5N]_3P{=}N{-}PCl_2$ [141.0(1)°]. The distances between the phosphorus atoms and the nitrogen atoms of the piperidino groups range from 1.622(3) Å to 1.640(2) Å and are similar to the values found for $[(CH_2)_5N]_3P{=}N{-}PCl_2$.

$[(Me_2N)_3P{=}N{-}P(NMe_2)_2Br]^+Br^-$

$[(Me_2N)_3P{=}N{-}P(NMe_2)_2Br]^+Br^-$ [45] crystallizes in the triclinic space group $P\bar{1}$ with two molecular units in the unit cell (Figure 5). As described for the vast majority of R_3PBr_2 compounds,[38b] $[(Me_2N)_3P{=}N{-}P(NMe_2)_2Br]^+Br^-$ exhibits an ionic structure instead of a pentacoordinate phosphorus atom. The molecular structure reveals a P2–Br1–Br2 angle close to linearity [171.32(2)°] and an anion-cation interaction with a Br···Br distance of 3.4774(3) Å, which is slightly below the sum of the van der Waals radii (3.66 Å).[44] This structural motif was also reported for $[Ph_3PBr]^+Br^-$ [Br···Br 3.123(2) Å],[46] $[Et_3PBr]^+Br^-$ [Br···Br 3.303(2) Å][38b] and $[i\text{Pr}_3PBr]^+Br^-{\cdot}0.5CH_2Cl_2$ [Br···Br 3.369(2) and 3.315(2) Å].[47] The Br···Br distance increases with the electron-donating properties of R_3P in the order $Ph_3P < Et_3P < i\text{Pr}_3P < ((Me_2N)_3P{=}N)(Me_2N)_2P$. The P–Br distance in $[(Me_2N)_3P{=}N{-}P(NMe_2)_2Br]^+Br^-$ [2.208(1) Å] is longer than observed in the literature-known structures {$[Ph_3PBr]^+Br^-$: 2.181(3) Å, $[Et_3PBr]^+Br^-$: 2.173(3) Å, $[i\text{Pr}_3PBr]^+Br^-{\cdot}CH_2Cl_2$: 2.185(3) and 2.174(3) Å}. This is a result of the electron rich $[(Me_2N)_3P{=}N{-}]$ substituent donating electron density into the σ*-P–Br bond, which is becoming less attractive for donation of the bromide donor Br2. As observed for the other two molecular structures discussed herein, the formal double bond P1–N4 [1.592(2) Å] is again longer than N4–P2 [1.551(2) Å].

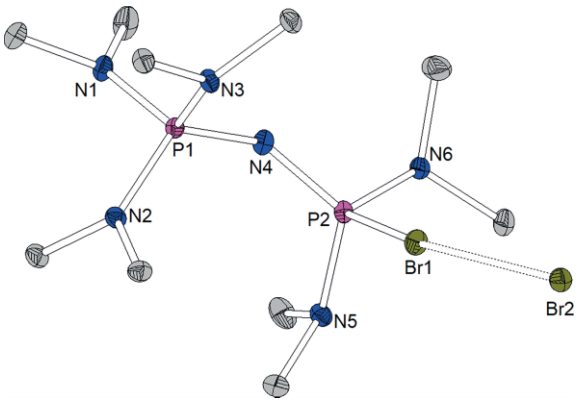

Figure 5. Molecular structure of $[(Me_2N)_3P{=}N{-}P(NMe_2)_2Br]^+Br^-$ (ellipsoids with 30% probability, hydrogen atoms are omitted for clarity). Selected bond lengths / and angles /°: P1–N1 1.630(2), P1–N2 1.632(2), P1–N3 1.638(2), P1–N4 1.592(2), N4–P2 1.551(2), P2–N5 1.650(2), P2–N6 1.636(2), P2–Br1 2.208(1), Br1··Br2 3.4774(3), P1–N4–P2 139.1(1), P1–Br1–Br2 171.32(2).

Computational Section

The gas phase proton affinity and gas phase basicity of phosphines **1**–**4** are calculated employing the ωB97XD/6-311+G(2df,p)//ωB97XD/6-31+G(d) theoretical model. The validity of this theoretical model is confirmed in a paper of *Bachrach*, where it was found that the ωB97XD functional provides more accurate values of gas phase proton affinity than M06–2X and/or B3LYP functionals.[48] The pK_{BH}^+ values in acetonitrile are calculated according to the approach of *Casasnovas* et al.[49] where a full geometry optimization in solution has been performed utilizing the CPCM solvation model. The Schwesinger base *t*Bu-P_2(dma)$_5$ (**5**) with an experimental pK_{BH}^+(MeCN) value of 33.49,[50] and the phosphine $P(CH_3)_3$ with a pK_{BH}^+(MeCN) value of 15.5[51] are applied as reference bases giving the corresponding calculated $pK_{BH}^+{}_{r1}$ $pK_{BH}^+{}_{r2}$ values. Herein, we will compare the basicity of *mono*-phosphazenyl phosphines **1**–**4** with *Dielmanns tris*-(1,3-diisopropyl-4,5-dimethylimidazolin-2-ylidenamino)-diisopropylphosphine with a calculated pK_{BH}^+(MeCN) of 38.8.[22,23] We also include the Verkade base $N(CH_2CH_2NMe)_3P$ (**6**)[52] into this basicity comparison. Calculated gas phase proton affinities, gas basicities and pK_{BH}^+(MeCN) values are given in Table 6.

Table 6. The calculated gas phase proton affinities (PA), gas phase basicities (GB), and pK_{BH}^{+} (MeCN) values [d] of phosphazenyl phosphines **1–4** and reference bases **5–7**. Values in square brackets are experimental results taken from the literature[50,51,17].

Molecules	PA P^{III}	(=N–)	GB P^{III}	(=N–)	pK_{BH}^{+} $pK_{BH}^{+}{}_{r1}$	$pK_{BH}^{+}{}_{r2}$
$(Me_2N)_3P{=}N{-}P(NMe_2)_2$ (**1**)	265.8	256.0	257.4	245.7	26.4	26.4
$[(CH_2)_4N]_3P{=}N{-}P[N(CH_2)_4]_2$ (**2**)	274.7	262.4	267.9	256.1	31.5	31.4
$[(CH_2)_5N]_3P{=}N{-}P[N(CH_2)_5]_2$ (**3**)	272.4	259.4	265.4	251.5	29.8	29.8
$[(CH_2)_6N]_3P{=}N{-}P[N(CH_2)_6]_2$ (**4**)	273.6	259.2	265.7	251.8	29.4	29.4
*t*Bu-P_2(dma)$_5$ (**5**)	–	277.2	–	269.3 [268.8] [a]	[33.49] [a]	33.5
Verkade-Me base (**6**)	263.1	–	256.0 [260.8] [a]	–		
$P(CH_3)_3$ (**7**)	230.9	–	223.6 [221.4] [c]	–	15.5	[15.5] [b]

a) Reference[50]. b) Reference[51]. c) Reference[17]. d) Values denoted by PIII are PA and GB values for protonation at the phosphorus atom, whereas (=N–) represent the values for protonation at the imine nitrogen atom. $pK_{BH}^{+}{}_{r1}$ and $pK_{BH}^{+}{}_{r2}$ are calculated utilizing *t*Bu-P_2(dma)$_5$ and $P(CH_3)_3$ as a reference bases, respectively.

Perusal of the data presented in Table 6 reveals that the most basic protonation site of the P_2 bases **1–4** is the phosphorus atom and not the phosphazenyl nitrogen atom (Scheme 8). Proton affinities for protonation at phosphorus are denoted by PA(P^{III}) whereas PAs where the imine nitrogen atom is protonated are denoted by PA(=N–). Protonation on the imine nitrogen atom gives PA values lower by 9.8–14.4 kcal·mol^{-1} than obtained for the protonation on the phosphorus atom. It appears that the calculated gas phase proton affinities and gas phase basicities of all investigated P_2 phosphines (**1–4**) exceed that of the paradigmatic Verkade proazaphosphatrane base $N(CH_2CH_2NMe)_3P$ (**6**). However, it should be noticed that the experimental and computational gas phase basicity for the Verkade base differs substantially (4.8 kcal·mol^{-1}). The difference is even larger if the B3LYP functional is employed. According to the B3LYP/6-311+G(2df,p)//B3LYP/6-31G(d) theoretical model, the PA and GB values of **6** are 261.0 and 252.8 kcal·mol^{-1}.[18] M062X/6-311+G(2df,p)//M062X/6-31G(d) gives by far the largest discrepancy compared to the experimental data, since the calculated PA and GB values obtained by this functional are 257.2 and 249.5 kcal·mol^{-1}, respectively (the error in GB value is 11.3 kcal·mol^{-1} (!). Considering that the DFT models mostly give PA and GB values in a good agreement with experimental ones, even for phosphines,[53] we decided to apply state-of-the-art ab initio G3B3 method to test whether the problem of discrepancy in GB value of **6** is associated with the inaccuracy of the DFT approach. The PA and GB values calculated utilizing the G3B3 method are 266.8 and 258.5 kcal·mol^{-1}, respectively. The GB value calculated utilizing G3B3 method is in much better agreement with the experiment which means that a higher level of theory should be employed for accurate basicity calculations of the Verkade base $N(CH_2CH_2NMe)_3P$. However, the latter is a specific phosphine where basicity increase occurs due to formation of a transannular P···N bond upon protonation. Possible failure in description of this bond could be the reason for large errors using DFT functionals. This phenomenon will be investigated in more detail in a future paper. Assuming that the Verkade base is a specific phosphine, and that ωB97XD gives accurate values for the PA and GB of the P_2 bases **1–4**, using the experimental GB value for **6**, we can conclude that **1** is less basic than **6**, whereas **2**, **3** and **4** are more basic in the gas phase. However, the basicity of **1–4** in solution is substantially lower than that of **6**. This needs some clarification. First of all, it should be mentioned that we obtained almost the same pK_{BH}^{+} values ($pK_{BH}^{+}{}_{r1}$ and $pK_{BH}^{+}{}_{r2}$) regardless if we utilized *t*Bu-P_2(dma)$_5$ or $P(CH_3)_3$ as reference base, which implies that the theoretical slope of 1/RTln(10) for the relation of the pK_{BH}^{+} value to ΔG is valid here.[54] Furthermore, the experimental pK_{BH}^{+}(MeCN) values of the Schwesinger base *t*Bu-P_2(dma)$_5$ and the Verkade base **6** are almost the same (the difference is only 0.1 unit), whereas the experimental GB of *t*Bu-P_2(dma)$_5$ is by 8 kcal·mol^{-1} higher than the GB of **6**. Since the basicity in solution represents the sum of the GB and the difference in Gibbs energy of solvation between the neutral base and the conjugate acid ($\Delta\Delta G_{sol}$), a higher pK_{BH}^{+} value for the Verkade base in comparison to *t*Bu-P_2(dma)$_5$ should be a consequence of a higher $\Delta\Delta G_{sol}$ value. This is indeed the case since the calculated $\Delta\Delta G_{sol}$ for *t*Bu-P_2(dma)$_5$ is 29.1 kcal·mol^{-1}, whereas for **6** the value of 36.9 kcal·mol^{-1} is obtained. The phosphines **1–4** possess a $\Delta\Delta G_{sol}$ similar to or slightly lower than that of *t*Bu-P_2(dma)$_5$ since the calculated $\Delta\Delta G_{sol}$ values are 30.1, 27.0, 26.5, 28.2 kcal·mol^{-1}, respectively. Therefore, although **2–4** are more basic than **6** in the gas phase, their pK_{BH}^{+} values in acetonitrile are lower. The lower $\Delta\Delta G_{sol}$ could be rationalized by a steric hindrance of the phosphorus atom due to the bulkiness of the $(R_2N)_3P{=}N{-}$ substituents in the case of **1–4** which prevents the access of the solvent molecules to the protonated phosphorus atom. In the Verkade base **6** this is not the case and the protonated phosphorus atom is more exposed to the solvent.

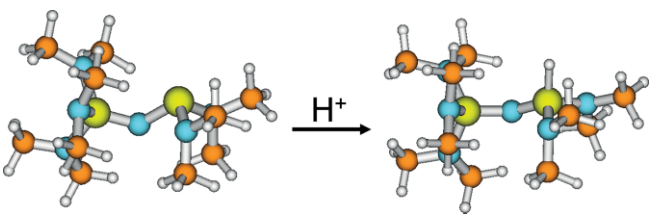

Scheme 8. Optimized gas phase structures of $(Me_2N)_3P{=}N{-}P(NMe_2)_2$ and $(Me_2N)_3P{=}N{-}P(NMe_2)_2{\cdot}H^{+}$.

According to the calculations, $(Me_2N)_3P{=}N{-}P(NMe_2)_2$, $[(CH_2)_5N]_3P{=}N{-}P[N(CH_2)_5]_2$, and $[(CH_2)_6N]_3P{=}N{-}P[N(CH_2)_6]_2$ exhibit by several order of magnitude higher pK_{BH}^{+} values on the acetonitrile scale than the

corresponding secondary amines dimethylamine, piperidine or azepane with experimentally measured pK_{BH^+} values around 19.[55] Since the basicity difference between the studied P_2 species and the corresponding secondary amines is relatively high in the gas phase and in acetonitrile solution, possible differences in crystal lattice energy, in Gibbs energy of solvation of ions, and in energy of ion pair formation in solution are responsible for the success of above mentioned syntheses applying amines as base and nucleophile.

Donor Strength of mono-PAPs

The donor strength of an electron donor depends on the nature of the acceptor. In this study, the electron-donor capabilities of selected mono-PAP $(dma)_3P{=}N{-}P(dma)_2$ (**1**) and $(Pyrr)_3P{=}N{-}P(Pyrr)_2$ (**2**) (dma = dimethylamino, Pyrr = pyrrolidino) were quantified by their Tolman electronic parameters (TEPs)[56] and their $^1J_{PSe}$ coupling constants[57] applying the same reference acceptors, $[Ni(CO)_3]$ and [Se], used in scaling up our tris-PAP $[(dma)_3P{=}N]_3P$ and $[(Pyrr)_3P{=}N]_3P$ (Table 7).[24]

Table 7. Donor capability measured as TEP [a] of $[L\text{-}Ni(CO)_3]$ complexes and as $^1J_{PSe}$ constants of selenides of mono-PAP **1** and **2** and references Verkade-Me base and tris-PAP.

	TEP /cm^{-1} [a]	$^1J_{PSe}$ /Hz [b]
$(dma)_3P{=}N{-}P(dma)_2$ (**1**)	2047.4	756
$(Pyrr)_3P{=}N{-}P(Pyrr)_2$ (**2**)	2042.4	735
Verkade-Me base [58,59]	2057.0	754
$[(dma)_3P{=}N]_3P$ [24]	2022.4	654
$[(Pyrr)_3P{=}N]_3P$ [24]	2018.6	628

a) Recorded via ATR-IR spectroscopy of neat substance. b) Recorded in $[D_6]$benzene.

For this purpose, **1** and **2** were reacted with $[Ni(CO)_4]$ and with grey selenium. Corresponding adducts [**1**-$Ni(CO)_3$], [**2**-$Ni(CO)_3$] as well as [**1**-Se] and [**2**-Se] were isolated and characterized. The higher the P-donor strength, the lower the TEP value, the frequency of the A1 C-O stretching mode, and the lower the $^1J_{PSe}$ coupling constant of their P-selenides.

On the TEP scale, the donor strength of the mono-PAP **1** and **2** is superior to that of Verkade-Me base.[58,59] It is in the range of 2050+5 cm^{-1} characteristic for classical NHCs or even stronger. On the NMR scale of corresponding selenides, the donor strength of Verkade-Me base is in between **1** and **2**, interestingly a similar trend as found in basicity. As expected mono-PAP do not keep up with the unrivaled donor strength of tris-PAP.

Conclusions

After having presented superbasic P_2-phosphazene chelates in previous publications, we shed light onto their mono-phosphazenylphosphine P_2-precursors within this work allowing insight into their facile and scalable synthesis, reactivity, spectroscopic properties, structural features, their basicity in solution and the gas phase, their nucleophilicity and donor strength. We are convinced that the amino-substituted P_2-nucleophiles and P_2-electrophiles presented here will be further used to synthesize P_2-phosphazene superbases with substituents other than classical NMe_2 and pyrrolidine groups. Furthermore, mono-PAP $(R_2N)_3P{=}N{-}P(NR_2)_2$ building blocks *per se* turned out to rival the basicity of commercially available Schwesinger diphosphazene $(Me_2N)_3P{=}N{-}P{=}NEt(NMe_2)_2$ (Et-P_2) and of Verkade's proazaphosphatrane superbases. They were used as readily available very strong P-nucleophiles in the synthesis of 1,8-naphthalene-bisphosphazides and as very strong P-donors rivaling the donor strength of classical NHCs in coordination chemistry.

Experimental Section

Reactions were carried out under inert atmosphere using standard Schlenk techniques. Moisture and air sensitive substances were stored in a conventional nitrogen-flushed glovebox. Solvents were purified according to literature procedures and kept under an inert atmosphere. Phosphorus trichloride was distilled prior to use. Pyrrolidine, piperidine and azepane were stirred over CaH_2 overnight and distilled prior to use. $P(N(CH_2)_4)_3$ was prepared by the reaction of PCl_3 with pyrrolidine in THF on the basis of a publication by *Dellinger* et al.[60] $P(N(CH_2)_5)_3$ was obtained in a similar procedure in ethyl ether, but purification was performed by precipitation from acetonitrile instead of distillation.[61] $P(N(CH_2)_6)_3$ was prepared via a transamination reaction of $P(NEt_2)_3$ with azepane.[62] Synthetic procedures of all new compounds and optimized ones of literature known $[(Me_2N)_3P{=}N{-}P(NMe_2)_2Br]^+Br^-$,[12,21] $[((CH_2)_4N)_3P{=}N{-}P(N(CH_2)_4)_2Br]^+Br^-$[8,9,12] and their corresponding precursors are presented in the Supporting Information.

Crystallographic data (excluding structure factors) for the structures in this paper have been deposited with the Cambridge Crystallographic Data Centre, CCDC, 12 Union Road, Cambridge CB21EZ, UK. Copies of the data can be obtained free of charge on quoting the depository numbers CCDC-977140, CCDC-1955686, and CCDC-1955687. (Fax: +44-1223-336-033; E-Mail: deposit@ccdc.cam.ac.uk, http://www.ccdc.cam.ac.uk)

Supporting Information (see footnote on the first page of this article): This includes synthetic procedures, NMR protonation experiments, NMR and IR spectra, crystallographic information and computational details.

Acknowledgements

We thank *Dr. Lars Finger* and *Dr. Fabian Schröder* for their valuable support with crystal structure refinement. Financial support by the bilateral DAAD – MZOS Academic Exchange Program between Germany and Croatia and financial support by the Fonds der Chemischen Industrie (doctoral scholarship for J·K.) is gratefully acknowledged. B.K. gratefully acknowledges support of the Computing Center of the University of Zagreb (SRCE) for granting computational time on ISABELLA cluster and CRO-NGI grid. Open access funding enabled and organized by Projekt DEAL.

Keywords: Basicity; Phosphines; Phosphazenes; Density functional calculations; Tolman electronic parameter

References

[1] R. Schwesinger, H. Schlemper, C. Hasenfratz, J. Willaredt, T. Dambacher, T. Breuer, C. Ottaway, M. Fletschinger, J. Boele, H. Fritz, D. Putzas, H. W. Rotter, F. G. Brodwell, A. V. Satish, G. Ji, E. Peters, K. Peters, H. G. von Schnering, L. Walz, *Liebigs Ann.* **1996**, 1055–1081.
[2] Y. Kondo, *Superbases for Organic Synthesis: Guanidines, Amidines and Phosphazenes and Related Organocatalysts* (Ed.: T. Ishikawa), John Wiley & Sons, Ltd., **2009**, pp 156–159.
[3] A. Solladié-Cavallo, B. Crescenzi, *Synlett* **2000**, 327–330.
[4] a) A. Solladié-Cavallo, A. Diep-Vohuule, T. Isarno, *Angew. Chem.* **1998**, *110*, 1824–1827; *Angew. Chem. Int. Ed.* **1998**, *37*, 1689–1691; b) A. Solladié-Cavallo, M. Roje, T. Isarno, V. Sunjic, V. Vinkovic, *Eur. J. Org. Chem.* **2000**, 1077–1080; c) A. Solladié-Cavallo, M. Roje, R. Welter, V. Šunjić, *J. Org. Chem.* **2004**, *69*, 1409–1412.
[5] A. J. Clark, Y. S. S. Al-Faiyz, D. Patel, M. J. Broadhurst, *Tetrahedron Lett.* **2001**, *42*, 2007–2009.
[6] H. Staudinger, J. Meyer, *Helv. Chim. Acta* **1919**, *2*, 635–646.
[7] A. V. Alexandrova, T. Mašek, S. M. Polyakova, I. Císařová, J. Saame, I. Leito, I. M. Lyapkalo, *Eur. J. Org. Chem.* **2013**, *9*, 1811–1823.
[8] J. F. Kögel, B. Oelkers, B. Kovačević, J. Sundermeyer, *J. Am. Chem. Soc.* **2013**, *135*, 17768–17774.
[9] J. F. Kögel, N. C. Abacılar, F. Weber, B. Oelkers, K. Harms, B. Kovačević, J. Sundermeyer, *Chem. Eur. J.* **2014**, *20*, 5994–6009.
[10] J. F. Kögel, D. Margetic, X. Xie, L. H. Finger, J. Sundermeyer, *Angew. Chem.* **2017**, *129*, 3136-3139; *Angew. Chem. Int. Ed.* **2017**, *56*, 3090 –3093.
[11] a) A. V. Kirsanov, *Izv. Akad. Nauk SSSR, Otd. Khim. Nauk* **1950**, 426; b) T. Rodima, V. Mäemets, I. Koppel, *J. Chem. Soc. Perkin Trans. 1* **2000**, 2637–2644.
[12] J. F. Kögel, N.-J. Kneusels, J. Sundermeyer, *Chem. Commun.* **2014**, *50*, 4319–4321.
[13] J. F. Kögel, B. Kovačević, S. Ullrich, X. Xie, J. Sundermeyer, *Chem. Eur. J.* **2017**, *23*, 2591–2598.
[14] H. M. Senn, D. V. Deubel, P. E. Blöchl, A. Togni, G. Frenking, *J. Mol. Struct.* **2000**, *516–558*, 233–242.
[15] A. A. Kolomeitsev, I. A. Koppel, T. Rodima, J. Barten, E. Lork, G.-V. Röschenthaler, I. Kaljurand, A. Kütt, I. Koppel, V. Mäemets, I. Leito, *J. Am. Chem. Soc.* **2005**, *127*, 17656–17666.
[16] I. A. Koppel, R. Schwesinger, T. Breuer, P. Burk, K. Herodes, I. Koppel, I. Leito, M. Mishima, *J. Phys. Chem. A* **2001**, *105*, 9575–9586.
[17] B. Kovačević, Z. B. Maksić, *Chem. Commun.* **2006**, 1524–1526.
[18] P. B. Kisanga, P. Ilankumaran, B. M. Fetterly, J. G. Verkade, *J. Org. Chem.* **2002**, *67*, 3555–3560.
[19] W. Su, S. Urgaonkar, P. A. McLaughlin, J. G. Verkade, *J. Am. Chem. Soc.* **2004**, *126*, 16433–16439.
[20] Z. Wang, B. Fetterly, J. G. Verkade, *J. Organomet. Chem.* **2002**, *646*, 161–166.
[21] A. P. Marchenko, G. N. Koidan, A. M. Pinchuk, A. V. Kirsanov, *Zh. Obshch. Khim.* **1984**, *54*, 1774–1782.
[22] M. A. Wünsche, P. Mehlmann, T. Witteler, F. Buß, P. Rathmann, F. Dielmann, *Angew. Chem.* **2015**, *127*, 12024–12027; *Angew. Chem. Int. Ed.* **2015**, *54*, 11857–11860.
[23] a) P. Mehlmann, C. Mück-Lichtenfeld, T. T. Y. Tan, F. Dielmann, *Chem. Eur. J.* **2017**, *23*, 5929–5933; b) F. Buß, P. Mehlmann, C. Mück-Lichtenfeld, K. Bergander, F. Dielmann, *J. Am. Chem. Soc.* **2016**, *138*, 1840–1843.
[24] S. Ullrich, B. Kovačević, X. Xie, J. Sundermeyer, *Angew. Chem. Int. Ed.* **2019**, *58*, 10335–10339; *Angew. Chem.* **2019**, *131*, 10443–10447.
[25] a) W. Wolfsberger, H. H. Pickel, H. Schmidbaur, *Z. Naturforsch. B* **1971**, *26*, 979–981; b) Ch. V. Reddy, J. V. Kingston, J. G. Verkade, *J. Org. Chem.* **2008**, *73*, 3047–3062; c) J. V. Kingston, J. G. Verkade, *J. Org. Chem.* **2007**, *72*, 2816–2822; d) N. L. S. Yue, D. W. Stephan, *Organometallics* **2001**, *20*, 2303–2308; e) S. Goumri, F. Lacassin, A. Baceiredo, G. Bertrand, *Heteroat. Chem.* **1996**, *7*, 403–408; f) E. P. Flindt, *Z. Anorg. Allg. Chem.* **1982**, *487*, 119–129.
[26] a) L. Birkofer, A. Ritter, P. Richter, *Chem. Ber.* **1963**, *96*, 2750–2757; b) D. W. Stephan, J. C. Stewart, F. Guerin, S. Courtenay, J. Kickham, E. Hollink, C. Beddie, A. Hoskin, T. Graham, P. Wei, R. E. v. H. Spence, W. Xu, L. Koch, X. Gao, D. G. Harrison, *Organometallics* **2003**, *22*, 1937–1947.
[27] H. Schmidbaur, W. Wolfsberger, *Angew. Chem.***1966**, *78*, 306–307; *Angew. Chem. Int. Ed. Engl.* **1966**, *5*, 312–313.
[28] a) W. Z. Wolfsberger, *Z. Naturforsch. B* **1978**, *33*, 1452–1456; b) S. Courtenay, C. M. Ong, D. W. Stephan, *Organometallics* **2003**, *22*, 818–825.
[29] O. Alhomaidan, C. Beddie, G. Bai, D. W. Stephan, *Dalton Trans.* **2009**, 1991–1998.
[30] J. Lorberth, *J. Organomet. Chem.* **1974**, *71*, 159–164.
[31] I. Kaljurand, T. Rodima, A. Pihl, V. Mäemets, I. Leito, I. A. Koppel, M. Mishima, *J. Org. Chem.* **2003**, *68*, 9988–9993.
[32] E. P. Flindt, H. Rose, H. C. Marsmann, *Z. Anorg. Allg. Chem.* **1977**, *430*, 155–160.
[33] O. Schlak, W. Stadelmann, O. Stelzer, R. Schmutzler, *Z. Anorg. Allg. Chem.* **1976**, *419*, 275–282.
[34] A. Eckart, K. Lux, K. Karaghiosoff, *Z. Anorg. Allg. Chem.* **2014**, 962–967.
[35] V. Raab, J. Kipke, R. M. Gschwind, J. Sundermeyer, *Chem. Eur. J.* **2002**, *8*, 1682–1693.
[36] B. Kovačević, Z. B. Maksić, *Chem. Eur. J.* **2002**, *8*, 1694–1702.
[37] K. Issleib, W. Seidel, *Z. Anorg. Anal. Chem.* **1956**, *288*, 201–215.
[38] a) H. Noeth, H. J. Vetter, *Chem. Ber.* **1965**, *98*, 1981–1987; b) S. M. Godfrey, C. A. McAuliffe, I. Mushtaq, R. G. Pritchard, J. M. Sheffield, *J. Chem. Soc., Dalton Trans.* **1998**, *22*, 3815–3818.
[39] a) H. Luo, G. A. Baker, J. S. Lee, R. M. Pagn, S. Dai, *J. Phys. Chem. B* **2009**, *113*, 4181–4183; b) S. Dai, H. Luo, G. A. Baker, U. S. Pat. Appl. Publ. **2011**, US 20110177428 A1 20110721.
[40] E. E. Nifantyev, M. K. Gratchev, S. Y. Burmistrov, M. Y. Antipin, Y. T. Struchkov, *Phosphorus Sulfur Silion Relat. Elem.* **1992**, *70*, 159–174.
[41] O. Dahl, *Tetrahedron Lett.* **1982**, *23*, 1493–1496.
[42] N. W. Mitzel, *J. Chem. Soc., Dalton Trans.* **1998**, 3239–3242.
[43] F. H. Allen, O. Kennard, D. G. Watson, L. Brammer, A. G. Orpen, R. Taylor, *J. Chem. Soc. Perkin Trans. 2* **1987**, S1-S19.
[44] M. Mantina, A. C. Chamberlin, R. Valero, C. J. Cramer, D. G. Truhlar, *J. Phys. Chem. A* **2009**, *113*, 5806–5812.
[45] This molecular structure has already been shown in the supporting information of reference [12] (CCDC number 977140).
[46] N. Bricklebank, S. M. Godfrey, A. G. Mackie, C. A. McAuliffe, R. G. Pritchard, *J. Chem. Soc., Chem. Commun.* **1992**, 355–356.
[47] F. Ruthe, W. W. du Mont, P. G. Jones, *Chem. Commun.* **1997**, 1947–1948.
[48] S. M. Bachrach, *J. Org. Chem.* **2013**, *78*, 10909–10916.
[49] a) R. Casasnovas, J. Ortega-Castro, J. Frau, J. Donoso, F. Muñoz, *Int. J. Quantum Chem.* **2014**, *114*, 1350–1363; b) R. Casasnovas, D. Fernández, J. Ortega-Castro, J. Frau, J. Donoso, F. Muñoz, *Theor. Chem. Acc.* **2011**, *130*, 1–13.
[50] I. Kaljurand, J. Saame, T. Rodima, I. Koppel, I. A. Koppel, J. F. Kögel, J. Sundermeyer, U. Köhn, M. P. Coles, I. Leito, *J. Phys. Chem. A* **2016**, *120*, 2591–2604.
[51] K. Haav, J. Saame, A. Kütt, I. Leito, *Eur. J. Org. Chem.* **2012**, 2167–2172.
[52] P. B. Kisanga, J. G. Verkade, *J. Org. Chem.* **2000**, *65*, 5431–5432.
[53] J.-N. Li, Y. Fu, L. Liu, Q.-X. Guo, *Tetrahedron* **2006**, *62*, 11801–11813.
[54] A. Klamt, F. Eckert, M. Diedenhofen, M. E. Beck, *J. Phys. Chem. A* **2003**, *107*, 9380–93806.
[55] a) I. Kaljurand, A. Kütt, L. Soovali, T. Rodima, V. Maemets, I. Leito, I. Koppel, *J. Org. Chem.* **2005**, *70*, 1019–1028; b) J. F. Coetzeel, G. R. Padmanabhan, *J. Am. Chem. Soc.* **1965**, *87*, 5005–5010.
[56] C. A. Tolman, *Chem. Rev.* **1977**, *77*, 313–348.

[57] W. McFarlane, D. S. Rycroft, *J. Chem. Soc., Dalton Trans.* **1973**, 2162–2166.
[58] Z. Thammavongsy, I. M. Kha, J. W. Ziller, J. Y. Yang, *Dalton Trans.* **2016**, *45*, 9853–9859.
[59] M. A. H. Laramay, J. G. Verkade, *J. Am. Chem. Soc.* **1990**, *112*, 9421–9422.
[60] D. J. Dellinger, D. M. Sheehan, N. K. Christensen, J. G. Lindberg, M. H. Caruthers, *J. Am. Chem. Soc.* **2003**, *125*, 940–950.
[61] J. L. Bolliger, O. Blacque, C. M. Frech, *Angew. Chem.* **2007**, *119*, 6634–6637; *Angew. Chem. Int. Ed.* **2007**, *46*, 6514–6517.
[62] L. A. Hussain, A. J. Elias, M. N. S. Rao, *Tetrahedron Lett.* **1988**, *29*, 5983–5986.

Received: March 3, 2020
Published Online: May 27, 2020

